Journal of the European Ceramic Society **15** (1995) 951–958

0955-2219(95)00073-9
0955-2219/95/$9.50

Grain Growth of Differently Doped Zirconia

J. A. Allemann,[a] B. Michel,[a] H.-B. Märki[a], L. J. Gauckler[a] * & E. M. Moser[b]

[a]Nonmetallic Materials, Swiss Federal Institute of Technology, CH-8092 Zürich, Switzerland
[b]EMPA, Überlandstr. 129, CH-8600 Dübendorf, Switzerland

(Received 13 September 1994; revised version received 26 March 1995; accepted 31 March 1995)

Abstract

Grain growth has been characterized for various zirconia alloys and cation segregations have been measured with AES and ESCA. The samples were prepared by coprecipitation, followed by compacting and sintering at 1400°C for different times. Grain growth was found to depend strongly on the dopants, e.g. on their radius and valence state. However, segregation factors of these cations did not reveal significant differences. Impurities up to 1 wt% are found to control grain growth via a grain boundary layer. Large amounts of Cr_2O_3 and SnO_2 tend to suppress grain growth effectively by the spherical shaped precipitations. The results are discussed in relation to the existing grain growth models.

Introduction

Polycrystalline tetragonal zirconia is a ceramic that combines both high strength and outstanding toughness, caused by a mechanism known as transformation toughening. One of the most important parameters for this toughening mechanism is the material's grain size. For good mechanical properties it must have a well defined value slightly smaller than a critical grain size being typically in the order of 1 μm for Y–TZP. In order to control grain growth in a ceramic body during processing, a profound knowledge of grain growth parameters is needed.

Grain growth of zirconia alloys depends very strongly on composition and is related to the phase content. The growth of cubic grains in zirconia doped with Y^{3+} is 30–250 times faster than that of tetragonal grains alloyed with the same cation.[1] Grain growth is strongly suppressed if both phases are coexistent. Furthermore it is well known, that Y^{3+} and Gd^{3+} suppress the grain growth very efficiently whereas Ce^{4+} does not. Up to now, the influence of a variety of alloying elements on the grain growth has been investigated, but there is still a strong controversy about the mechanisms involved in this process.

Two models are proposed up to now. **Model 1**: Theunissen *et al.*[2] proposed a solute drag model based on the observed enrichment of Y^{3+} at the surface of both Y–TZP and Y–FSZ. Hwang and Chen[3] confirmed this observation qualitatively and explained the segregation behavior of different dopants using a space charge concept. **Model 2**: Based on the large differences in Y_2O_3 content from grain to grain during sluggish partitioning, Lange *et al.*[4] suggested that coherency strains arise when boundaries between grains with different compositions move, suggesting one possible correlation between sluggish phase partitioning and slow grain growth. Stoto, Nauer and Carry[5] confirmed the sluggish grain growth during phase partitioning and observed an enhanced grain growth after phase segregation had occurred.

There are still some discrepancies in both of these models. **Model 1**: Hwang and Chen[3] found an enrichment factor for Y^{3+} of 1·9 whereas a much stronger enrichment factor of 4·3 has been found by Theunissen. On the other hand, Nauer and Carry found yttria segregation at grain boundaries only in combination with a 2 nm thick amorphous intergranular phase. The influence of such a glasslike layer on the segregation of dopants is said to be negligible by Hwang and Chen and not taken into consideration by Theunissen.[6,7] **Model 2**: The most significant decrease in grain growth occurs generally with concentrations up to the solubility limit. Model 2 cannot explain the strong decrease of grain growth within the homogeneity range, as there is no compositional difference between the grains. In addition, it is difficult to explain with Model 2 the observation that the grain growth of samples within the two phase field is approximately constant. This in spite of the fact, that the compositional inhomogeneities might increase with increasing dopant concentration.

*To whom correspondence should be addressed.

The aim of this study was to investigate the influence of alloying elements on the grain growth of tetragonal zirconia and based on these results to differentiate between the validity of the different models.

Experimental

Sample preparation and characterization

Doped zirconia powders were made by coprecipitating $ZrOCl_2 \cdot H_2O$ (Corustar, Frankfurt, D) and metal chlorides (Fluka AG, grade p.a.) in aqueous solutions with ammonia. The filtered hydroxides were washed chlorine free, spray dried and calcined at 700°C for 1 h. Finally these powders were attrition milled at 1500 rpm for 30 min and again spray dried. The commercial powder 6 Y–ZrO_2 (Alusuisse-Lonza Services AG, P021) has been fabricated with a similar technique, but calcined at 750°C for 8 h. For explanation: an alloy 3 7 AB–ZrO_2 has the composition 3 ct% A^{a+}, 7 ct% B^{b+} and 90 ct% Zr^{4+} (ct% = cation%). Solely the grain growth experiment at 1550°C was carried out with an other 6Y–ZrO_2 powder (Tosho, Tokio, Japan; TZ-3YB/PVA).

All powders were pressed uniaxially to cylinders (Ø15 mm, h ≈ 8 mm) without adding any binder and compressed isostatically at 250 MPa. Subsequently they were heated with 10 K/min to 1400°C and sintered for 5 min or 8, 24 or 72 h, respectively. Afterwards they were quenched in air down to room temperature.

The phases in the sintered samples were analyzed with a X-ray diffractometer (D 5000, Siemens). The diffraction patterns were collected with Cu Kα radiation (γ = 1·5405 Å) over an angular range of 10–80° 2θ. Those samples which disintegrated during cooling were ground and measured in powdered form. Measurements have been carried out on the uncracked samples before and after removing a surface layer by polishing; no change in the m : t : c phase ratio has been found between bulk and layers.

The grain size has been measured on fracture surfaces with a scanning electron microscope (SEM) and evaluated based on the mean intercept method. The results were fitted with the phenomenological equation:

$$D^n - D_o^n = kt \quad (1)$$

In this equation, grain size D depends on the starting grain size D_o, the exponential parameter n, the preexponential factor k and the time t. The exponent n depends on the microstructure.[8] Therefore, the data were evaluated for both n = 2, and n = 3. In addition, the best fitting n was determined for each material using an approximation algorithm. No significant difference could be found between these methods. In order to be able to compare the different grain growth coefficients k to each other and to published data, it has been fixed at n = 3.

Segregation measurements

Scanning electron images (SEI) and depth profiles on inter- and intracrystalline fractures at the selected areas of <0·01 μm^2 have been performed with a Perkin Elmer PHI Model 4300 SAM spectrometer operating with a primary beam energy of 3 kV and an electron beam current of 0·01 μA. Small pieces of the ceramic samples were pressed into a gold foil and heated up to 450°C by resistivity in order to enhance the electrical conductivity of the material while its thermal stability is still maintained.[9] A residual pressure lower than $9–10^{-10}$ mbar has been maintained in the analytical chamber during the measurements. The sensitivity factors of the oxides[6,7] have been used to calculate the cation's concentration with the exception of calcium,[10] where that of the oxide is unknown. The ion gun was operated with an Ar^+ ion energy of 2 keV, corresponding to an etching rate of 0·93 nm/min with an interface resolution of 2·8 nm for a 33 nm SiO_2/Si (111) standard reference which corresponds to a sputtering rate of 0·46 nm/min for a ZrO_2/Si (111) reference.

Photoelectron spectroscopy measurements have been recorded with a Perkin Elmer PHI 5400 small spot ESCA apparatus equipped with a channel plate detector and a Mg X-ray source operated at 400 W (15 kV; 26,7 mA). The pass energy of the analyzer has been set to 35·75 eV, resulting in a full width at half-maximum (FWHM) value of 1·0 eV for the Ag($3d_{5/2}$) line. The Zr($3d$) line at 182·2 eV was used as a reference to correct for sample charging.[11]

Generally, AES and XPS concentration measurements agreed only roughly with chemically determined concentrations. The estimation of errors of the measured concentrations takes only those errors into account which are due to uncertainties of data evaluation. Several factors can cause additional deviations. It was not possible to hold the incidence angle between the electron beam and different grains' surfaces constant. The deviations amount to about ±10°. Therefore, the information depth of the investigated layer varies and so does the measured cation concentration. By changing this angle, the concentration was found to alter in the order of ±3 ct%. The quantitative analysis of Y(MNN) and Ce(MNN) was difficult to perform due to a peak overlapping with Zr(MNN). If only the first half of the Y(MNN) AES-peak was taken

into consideration and this concentration was multiplied with 2, influences of the overlapping Zr(MNN)-lines could be excluded. The XPS signals were merely integrated and no deconvolution has been carried out. For such an evaluation Ce(MNN) concentrations of AES and XPS measurements showed similar results. During the enhanced exposure of the grains to the electron beam, a loss of calcium was observed. In case of Ti, Ce, Y and Zr, the sensitivity factors of the oxides have been used to calculate the cation's concentrations.[6,7] Excluding preferential sputtering,[12] the measured concentrations are compatible to the concentrations determined by chemical analysis. Since the sensitivity factor of CaO was not available, that of the metal has been taken; the absolute concentrations of the titanium is also affected. Thus, these values are not comparable with chemically determined concentrations and can be regarded just relatively to each other.

Results and Discussion

Grain growth of differently doped zirconia

Grain size of differently doped zirconia has been measured as a function of soaking time at 1400°C (Fig. 1). The grain size D increases with the soaking time t according to a law, best described by eqn (1). Undoped tetragonal ZrO_2 at 1400°C has a grain growth coefficient $k = 2{\cdot}4 \times 10^{-22}$ m^3/s. The grain growth is enhanced by doping with smaller cations whereas it becomes sluggish by doping with larger ones (Table 1). In addition, the grain growth is more effectively suppressed by large cations, if they have a lower valence state. That explains why Ce^{4+} suppresses the grain growth only weakly whereas the grain growth slows down significantly by doping with Gd^{3+} and Y^{3+}. The same relationship has been demonstrated by Hwang and Chen[2] for 12 Ce–ZrO_2 doped with ternary cations of different size and valence state. Their grain growth coefficients k are slightly larger than ours due to the smaller concentration of doping cations. However, their data depends on both the size as well as the valence of the doping cation. k factors as small as $0{\cdot}01 \times 10^{-22}$ m^3/s to $0{\cdot}02 \times 10^{-22}$ m^3/s were found for Y–TZP. This extreme grain growth suppression had not been observed in the other alloying systems.

Table 1. Grain growth coefficients k of eqn 1 and $n = 3$ for alloyed tetragonal ZrO_2 at 1400°C in units of 10^{-22} m^3/s

Valence	*Ionic size: smaller than Zr^{4+}*	*Ionic size: larger than Zr^{4+}*
	For pure ZrO_2	2·4
2^+	MgCe: 1†	CaCe: 0·3†
		Y: 0·02
3^+	Cr: 12	(0·12 at 1500°C, 0·49 at 1550°C)
		Y: 0·01...0·02*
		Gd: 0·1 #
		YCe: 1...2†
		RECe: 1...3†
4^+	Ti: 17	Ce: 1·2

†Ref. 3: Grain growth at 1420°C was measured in a ternary systems by adding 1ct% of a dopant to 12 Ce–ZrO_2.
*Ref. 22: 1400°C, Ref. 5: 1450°C.
Ref. 13: 1400°C.

Y–TZP has been annealed at different temperatures. The grain growth coefficients k of Y–TZP were found to be 0·02, 0·12 and $0{\cdot}49 \times 10^{-22}$ m^3/s at 1400, 1500 and 1550°C, respectively. The study was done more carefully at 1550°C up to 300 h (Fig. 2) as the mechanical properties generally are tailored at this temperature. No increased grain growth has been observed at all during and after the partitioning of an oversaturated tetragonal phase to stable (t + c) phases (a phase analysis has not been carried out, but the long annealing times at 1550°C suggest an extensive progress in phase partitioning). This is in clear contradiction to

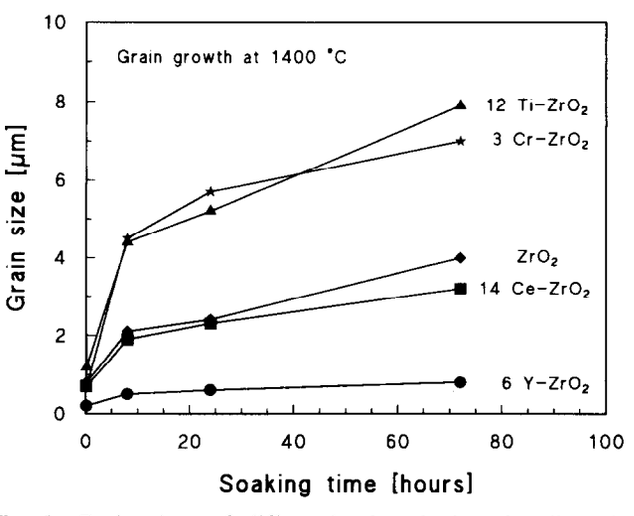

Fig. 1. Grain sizes of differently doped zirconia alloys in function of the annealing time at 1400°C.

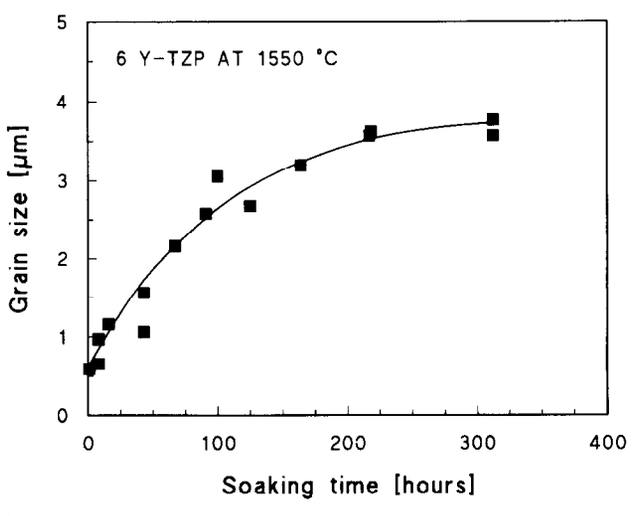

Fig. 2. Grain sizes of 6 Y–TZP as a function of the soaking time at 1550°C.

observations made by Nauer *et al.*[5] at 1400 and 1450°C up to 200 h. It is assumed that their findings are caused by another unknown growth mechanism. Our results suggest that phase partitioning has at least not a strong influence on grain growth.

Solid solutions of zirconia with 6, 10 and 12 ct% Ti^{4+} have been prepared using the described coprecipitation method. The grain growth of the annealed samples resulted in k values of 16·9, 16·7 and 16·2 10^{-22} m^3/s, respectively. This suggests that grain growth does not depend on the concentration within the investigated range. It is therefore assumed that the grain growth of zirconia doped with small cations is concentration independent above a threshold value which up to now is not known. In addition, zirconia doped with 3 ct% Cr^{3+} has a grain growth coefficient k = 12·3 10^{-22} m^3/s, which is not significantly different from that found in the samples Ti–ZrO_2. In contrast, Gd^{3+} inhibits the grain growth effectively up to a concentration of 1·5 ct%[13] (Fig. 3), which is close to the solid solubility limit of 1·1 ct%. The decrease of the grain growth in the homogeneity range is inverse proportional to the concentration as predicted by the solute drag model of Lücke.[14] In the two phase regions, the grain growth is pretty much constant. A similar behavior has been found also in other systems such as in Y–ZrO_2,[15] La–ZrO_2,[16] Ca–ZrO_2[3] and YCe–ZrO_2.[17]

The above results suggest that cations smaller than Zr^{4+} increase the grain growth, independent on both their concentration and valence. In contrast, larger cations suppress it very strongly. Grain growth coefficients decrease mainly within the homogeneity range and do not depend on the concentration in the two phase region. Our results do not give evidence for a enhanced grain growth during or after the phase partitioning process.

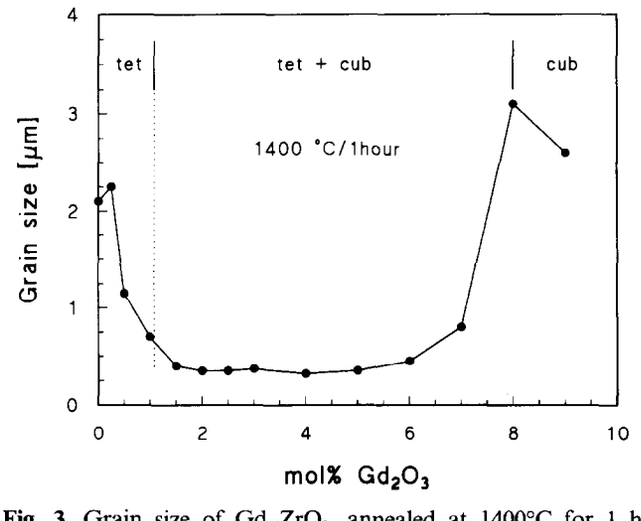

Fig. 3. Grain size of Gd–ZrO_2, annealed at 1400°C for 1 h as a function of the Gd^{3+} concentration (after Leung *et al.*)[13]

Therefore it is proposed that phase partitioning has not an essential influence on grain growth.

Segregation of dopants

Segregations of doping cations within a zirconia grain have been investigated using AES (Auger Electron Spectroscopy) and XPS (X-ray Photoelectron Spectroscopy). Surface concentrations have been ascertained on several intercrystalline broken grain facets. The observed concentrations reveal the same tendencies and are reproducible within some ct%, governed by the resolving limit of the applied method. Concentration profiles have been worked out by sputtering off layer by layer up to the grains' interior. For some samples it was possible to confirm these bulk concentrations by AES measurements on transcrystalline fracture faces. The obtained values agreed well to each other. Concentration measurements of Ca^{2+} are not compatible with values obtained from chemical analysis, as the sensitivity factor of the oxide is unknown and thus that of the metal had to be taken. Therefore, these results can be regarded just relatively to each other.

The surface and bulk concentrations were used to determine the segregation factors of the different dopants (Table 2). They are summarized briefly in the following:

Y^{3+} has a segregation factor of 2·4. The enrichment of Y-ions is observed in the uppermost layers at the surface of the grains. The surface concentration has been confirmed on several grains.

Ti^{4+}: In all binary alloys as well as in the ternary sample 7 8 CeTi–ZrO_2, the Ti^{4+} has a segregation factor of about 5. Furthermore it has been observed, that the segregation generally occurs within a broad layer, extending up to 6 nm into the grain. In a ternary alloy together with Ca^{2+}, segregation of Ti^{4+} clearly is less pronounced.

Ce^{4+} has a segregation factor of 2·2. This factor does not change significantly in ternary alloys with titanium oxide.

Ca^{2+}: The determined surface and bulk concentrations of these alloys are much too high. One explanation is, that this discrepancy is caused because the sensitivity factor of the metal is used rather than that for the oxide. We exclude that our data are collected on possible second phases, because the same values were also gathered on X-ray single phase materials. Whatever originated this error, the segregation factor of Ca^{2+} should not be affected significantly. It has been determined to about 1·5 for both the binary and ternary alloy and has been confirmed on other alloys as well.

Table 2. Concentrations of various cations at the surface (C_s) and in the bulk (C_b) and the resulting segregation factors C_s/C_b for zirconia alloys

Sample	C_s *(cat%)*	C_b *(cat%)*	*Thickness (nm)*$^+$	C_s/C_b	*Method*
6 Y–ZrO_2	19±1	8±1	1	2·4	AES/XPS
6 Ti–ZrO_2	43·1±0·6	8·1±1·8	6	5·3	AES
12 Ti–ZrO_2	47·3±0·6	9·6±1·8	6	4·9	AES
14 Ce–ZrO_2	22±4	10±3*	2	2·2	AES/XPS
7 8 CeTi—ZrO_2	11±3 Ce	4±3 Ce	2	2·8	AES/XPS
	45·2±0·5 Ti	11·2±1·8 Ti	3	4	
17 Ca–ZrO_2 (c)♦	51·3±0·2	34·9±0·4	2	1·5	AES
6 8 CaTi–ZrO_2♦	33·3±0·6 Ca	25·5±1·2 Ca*	1	1·3(Ca)	AES
	28·7±0·6 Ti	20·3±1·8 Ti*	3	1·4(Ti)	

*Confirmed on transcrystalline fracture faces: 26·9 (1·2) ct% Ca, 17·2 (1·7) ct% Ti.
♦Sensitivity factor of Ca-metal was taken rather then that of the oxide. See test for explanation.
$^+$Thickness of the segregation zone.

Segregation factors for all doping cations vary between 1 and 5·3 and seem to be relatively small for those cations which suppress grain growth and large for those which promote it. In addition, the segregation factors may not depend strongly on the dopant's concentration (Ti–ZrO_2). Furthermore, the segregation factor of Ti^{4+} is altered by alloying Ti–ZrO_2 with Ca^{2+} (6 8 CaTi–ZrO_2), but it appears not to be affected by Ce^{4+}, e.g. in the alloy 7 8 CeTi–ZrO_2. This behavior might be explained by the formation of an overcoat as mentioned by Theunissen *et al.*[6] The cations of titanium and cerium do form such an overcoat, i.e. behave in a similar way, but not that of calcium.

The segregation factors of Ce^{4+}, Ti^{4+} and Ca^{2+} in all binary and ternary alloys do not change markedly with increasing cation concentration, but the surface concentration of these cations increase if the bulk concentration is enhanced. This is consistent with the measurements of Hwang and Chen,[3] but not with those of Theunissen,[6,7] who found a constant Y^{3+} enrichment at the surface for all investigated concentrations.

Segregation factors of Ca^{2+} do not change strongly between tetragonal (at the time of soaking) and cubic grains. Similar segregation factors in these two crystal structures have also been found by Theunissen *et al.*[6,7] for yttria doped zirconia. Nevertheless, the grain growth of the tetragonal and cubic single phase microstructures are clearly different. This is surprising because the cation's segregation barrier cannot be responsible for such a large difference. One possible explanation is that lattice misfits between randomly oriented tetragonal grains inhibit grain growth. The lattice parameters of two touching grains are different and must be changed abruptly if one of that grains is growing into the other. Such lattice misfits do not exist in cubic grains and their grain growth is therefore faster.

The above results support therefore the idea that the segregation factors are similar for all cations in binary and ternary zirconia alloys. No evidence has been found for the suggestion of Hwang *et al.*,[3] that cations with a larger effective charge are more strongly attracted to the grain boundary than others. However, it is well known that cations alter diffusion significantly by their size and valence. The segregation of slowly diffusing cations thus is able to pin a grain boundary whereas the equally strong segregation of fast diffusing cations cannot do this.

Grain growth of polyphase zirconia

Second phases alter the grain growth of doped zirconia significantly. Main parameters are their mobilities, concentrations and morphologies. It is demonstrated in the following, that impurities influence the grain growth in a fundamentally different manner than second phases in amounts exceeding few mol%.

Impurities of SiO_2 and Al_2O_3 up to 1 wt% are added in various ratios to Y–TZP (Table 3(a)). The applied processing procedure is described in Ref. 18. Generally, it is found that increasing amounts of impurities lead to increased grain growth coefficients k (Fig. 4(a)). However, in the sample doped with only SiO_2, grain growth was insensitive to the amount of added SiO_2. By mixing SiO_2 and Al_2O_3 in a ratio of 1 : 1, abnormal grain growth was observed, leading to grains 10 times larger than those of the matrix. The resulting k value, evaluated merely based on the small matrix grains, does not reflect a proper grain growth mechanism and thus cannot be compared with the normal grain growth coefficients of the other samples.

Insoluble impurities have an impact on grain growth mainly by forming a grain boundary phase (Fig. 4(b)). The thickness of such grain boundaries has been measured by Impedance Spectroscopy

Table 3 (a) Grain growth coefficients k of Y–TZP with impurities of varying $SiO_2 : Al_2O_3$ ratios. (b) Grain growth coefficients k of zirconia alloys with large amounts of second phases and the characteristics

(a)

$SiO_2 : Al_2O_3$	$SiO_2 + Al_2O_3$ (wt%)	$k/10^{-22}$ (m^3/s)	δ_{GB} (nm)
0:0	<0·03	0·12	0·04
1:0	0·92	0·06	0·33
4:0	0·96	0·36	5·23
1:1	0·48	0·30	2·48
1:4	0·72	0·36	1·88
0:1	0·95	0·18	0·31

(b)

Sample	$k/10^{-22}$ (m^3/s)	Correlation r	Solubility	Precipitations	Morphology
ZrO_2	2·42	0·990		No	
3 Cr–ZrO_2	12·3	0·97		Nearly none	
10 Cr–ZrO_2	0·42	0·96	Cr: 1·4[23]	Cr_2O_3	*
12 Cr–ZrO_2	0·06	0·65		Cr_2O_3	*
5 In–ZrO_2	0·24	0·97	In: 3·4[24]	In_2O_3	#
6 8 CaTi–ZrO_2	2·25	0·997	Ca: 5[25]	M + c	
9 8 CaTi–ZrO_2	0·63	0·98	Ti: 15[26]	M + c + CZ	
10 15 CaTi–ZrO_2	7·19	0·996		M + c + CZ + ZT	
5 Bi–ZrO_2	34·5	0·95	Bi: 0[21]	Bi_2O_3	*
10 Sn–ZrO_2	1·2	0·98	Sn: ?	SnO_2	*

CZ: $CaZr_4O_9$, ZT: $ZrTiO_4$.
*Spherical, in triple points.
#Enlongated crystals.

and evaluated with a 'brick layer model' described elsewhere.[19] High purity Y–TZP has no grain boundary layer (0·04 nm) and a grain growth coefficient of k = 0·12 10^{-22} m^3/s, both determined on samples annealed at 1500°C. The addition of pure SiO_2 or Al_2O_3 lead in both cases to 0·3 nm thin grain boundary layers. In spite of that similarity, these layers alter the grain growth differently, namely they suppress it by SiO_2 and enhance it by Al_2O_3 additions. This behavior is surprising as SiO_2 is thought to form a viscous layer whereas Al_2O_3 is known as unyielding. However, due to the high annealing temperature of 1500°C, the formation of $ZrSiO_4$ is plausible. Due to the small dimension of its layer, the composition could not be determined. Mixed SiO_2–Al_2O_3 impurities caused much thicker grain boundaries as well as enhanced grain growth. The thickness of the grain boundary layers increased with increasing $SiO_2 : Al_2O_3$ ratio.

The viscosity of the grain boundary layer dominates the influence on grain growth. Due to the lack of viscosity data, the latter can be estimated with the help of melting temperatures T_M. Based

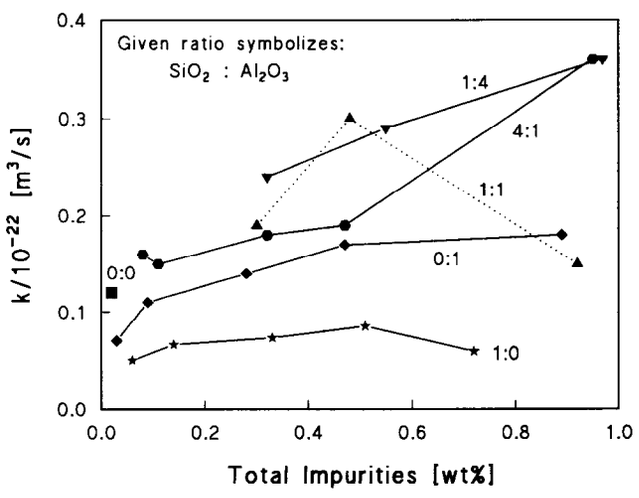

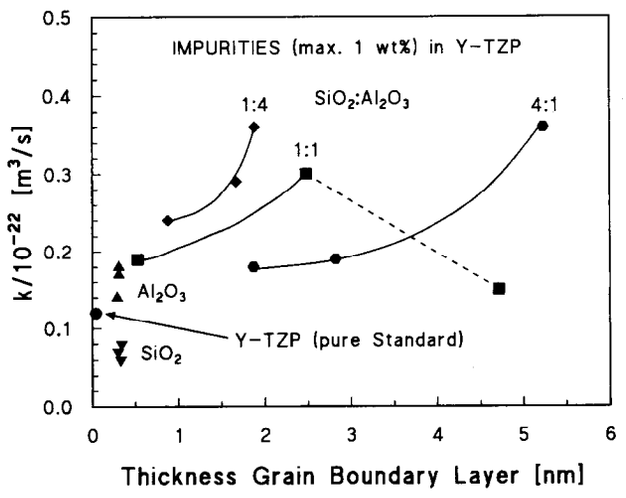

Fig. 4. (a) Grain growth coefficients k of Y–TZP containing up to 1 wt% impurities such as Al_2O_3, SiO_2 or mixtures of both as a function of the total amount of the impurities (Al_2O_3 + SiO_2). (b) Grain growth coefficients k as a function of the grain boundary layers formed.

on the ternary Y_2O_3–SiO_2–Al_2O_3 phase diagram,[18] the following relations are found: $T_{M,1:0}$ (liquidus of $ZrSiO_4$) > $T_{M,0:1}$ > $T_{M,1:4}$ > $T_{M,1:1}$ > $T_{M,4:1}$. The grain growth is enhanced in the same sequence.

If considerable amounts of a second phase are present, precipitations rather than grain boundary phases become crucial for grain growth. The grain growth coefficients k were determined for several systems containing large amounts of second phases (Table 3) and their influence could roughly be estimated. Chromium oxide in solid solution increases the grain growth but its precipitation decreases k by a factor of 200, despite the fact that chromium starts to volatilize around 1400°C. The same holds qualitatively also for tin oxide. 6 8 CaTi–ZrO_2 contained at room temperature substantial portions of monoclinic (at 1400°C tetragonal) and just few % cubic grains. Its grain growth is comparable to that of pure zirconia. The addition of 3 mol% more Ca^{2+} results in the formation of $CaZr_4O_9$. The grain growth is clearly suppressed by this second phase. Increase of the titanium oxide concentration to 7 mol% results in the formation of an additional $ZrTiO_4$ phase, i.e. the sample now contains 4 different phases. The grain growth of this sample is strongly increased, indicating a grain growth accelerating influence of $ZrTiO_4$. Bismuth additions increased the grain growth, too. This behavior must be caused by forming mobile Bi_2O_3 precipitations in triple points (as observed by SEM) and by a volatile phase. The large radius of Bi^{3+}, its valence and its low solubility[21] exclude a grain growth accelerating influence in solid solution of zirconia.

In summary, SiO_2 impurities probably in form of $ZrSiO_4$ decrease the grain growth whereas large amounts of SiO_2 increase it. In contrast, Al_2O_3 impurities enhance grain growth only slightly, whereas large amounts suppress it very efficiently. Cr_2O_3 and SnO_2 inhibit grain growth very efficiently but they evaporate at temperatures around 1400°C. These findings suggest that impurities influence grain growth over a grain boundary layer whereas larger amounts of a second phase control grain growth based on its morphology, mobility and amount.

Conclusions

Grain growth is found to be varied by the doping cations up to a factor of 10.[4] Large, low valence cations are most effective to reduce grain growth in agreement with the solute drag model whereas small ones increase it independent of their valence state and concentration. The cations' segregations are similar for all investigated alloys and do not reveal any correlation with the grain growth coefficients k. It is therefore suggested that segregations generally occur independent of the cations valence state, e.g. not with a space charge mechanism. However, the pinning of the grain boundaries is most effective in alloys doped with large cations of low valence, indicating, that the diffusion of the segregated cations is the controlling mechanism. The grain growth behavior of Y–TZP is not altered during and after phase partitioning, excluding it as a growth controlling mechanism. Impurities were found to govern grain growth by forming grain boundary layers, whereas larger amounts of a second phase controls the grain growth by mobility, morphology and amount of the precipitations. Thus, SiO_2 impurities (probably in form of $ZrSiO_4$) decrease the grain growth whereas large amounts increase it. In contrast, Al_2O_3 impurities increase grain growth, whereas considerable amounts of it suppress it very efficiently. Furthermore, grain growth could be suppressed by spherical Cr_2O_3– and SnO_2-precipitations.

Acknowledgements

We are grateful to Prof. Dr G. Bayer for his suggestions and helpful discussions. This study was partially supported by Alusuisse-Lonza Services Ltd.

References

1. Lee, I., Sintering and grain growth in tetragonal and cubic zirconia, Dissertation, University of Michigan, 1990.
2. Theunissen, G, Winnubst, A. & Burggraaf, A., Segregation aspects in the ZrO_2–Y_2O_3 ceramic system, *J. Mat. Sci. Lett.*, **8** (1989) 55–7.
3. Hwang, S. & Chen, I., Grain size control of tetragonal zirconia polycrystals using the space charge concept, *J. Am. Ceram. Soc.*, **73**(11) (1990) 3269–77.
4. Lange, F., Marshall, D. & Porter, J., Controlling microstructures through phase partitioning from metastable precursors: the ZrO_2–Y_2O_3 System. In *Ultrastructure Processing of Advanced Ceramics*, eds J. Mackenzie & D. Ulrich. Wiley, New York, 1988, pp. 519–32.
5. Stoto, T., Nauer, M. & Carry, C., Influence of residual impurities on phase partitioning and grain growth processes of Y–TZP materials, *J. Am. Ceram. Soc.*, **74**(10) (1991) 2615–21.
6. Theunissen, G., Microstructure, fracture toughness and strength of (ultra)fine-grained tetragonal Zirconia ceramics, Dissertation der Universität Tweente, Niederland, Februar 1991.
7. Theunissen, G., Winnubst, A. & Burggraaf, A., Surface and grain boundary analysis of doped zirconia ceramics studied by AES and XPS, *J. Mat. Sci.*, **27** (1992) 5057–66.
8. Brook, R., Controlled Grain Growth. In *Treatise on Materials Science and Technology*, Vol. 9, Ceramic Fabrication Processe, Academic Press (1976) 331–64.

9. Hamminger, R., SIA, **12** (1988) 519–26.
10. Davis, L., MacDonald, N., Palmberg, P., Riach, G. & Weber, R., *Handbook of Auger Electron Spectroscopy*, Perkin Elmer Corporation, Eden Prairie, (1979).
11. Hughes, A. & Sexton, B., *J. Mater. Sci.*, **24** (1989) 1057.
12. Moser, E. M., Metzger, M. & Gauckler, L. J., SAM/AES Analysis of Grain Boundaries in Zirconia Ceramics, submitted to *Fresenius' J. Anal. Chem.*, **8** Working conference on applied surface analyses, Kaiserslautern (1994).
13. Leung, D., Chan, C., Rühle, M. & Lange, F., Metastable crystallization, phase partitioning, and grain growth of ZrO_2–Gd_2O_3 materials processed from liquid precursors, *J. Am. Ceram. Soc.*, **74**(11) (1991) 2786–92.
14. Lücke, K., Rixen, R. & Rosenbaum, F., The impurity drag theory. In *The nature and behavior of grain boundaries*, ed. H. Hu, Plenum Press, 1972, p. 256–73.
15. Lange, F., Transformation-toughened ZrO_2: correlations between grain size control and composition in the system ZrO_2–Y_2O_3, *J. Am. Ceram. Soc.*, **69**(3) (1986) 240–2.
16. Bastide, B., Odier, P. & Coutures, J., Phase equilibrium and martensitic transformation in lanthana-doped zirconia, *J. Am. Ceram. Soc.*, **71**(6) (1988) 449–53.
17. Duh, J. & Lee, M., Fabrication and sinterability in Y_2O_3–CeO_2–ZrO_2, *J. Mat. Sci.*, **24** (1989) 4467–74.
18. Michel, B., Korngrenzenglasphasen in tetragonalem Zirkonoxid, Diss. ETH Nr. 10247.
19. Gödickemeier, M. *et al.*, Effect of intergranular glass films on the electrical conductivity of 3Y–TZP, *J. Mater. Res.*, **9**(5) (1994) 1228–40.
20. Bondar, I. A. & Galakhov, F. Y., Phase equilibria in the system Y_2O_3–Al_2O_3–SiO_2, *Izv. Akad. Nauk. SSSR, Ser. Khim*, **7** (1964) 1231–2.
21. Tcheichvili, L. & Marques, M., Systeme ZrO_2–Ti_2O_3, ZrO_2–In_2O_3 und ZrO_2–Bi_2O_3, *Keramische Zeitschrift*, **33**(5) (1982) 294.
22. Nieh, T. & Wadsworth, J., Dynamic grain growth during superplastic deformation of yttria-stabilized tetragonal zirconia polycrystals, *J. Am. Ceram. Soc.*, **72**(8) (1989) 1469–72.
23. Jayaratna, M. & Yoshimura, M., Hot pressing of Y_2O_3–stabilized ZrO_2 with Cr_2O_3 additions, *J. Mat. Sci.*, **21** (1986) 591–6.
24. Sasaki, K., Bohac, P. & Gauckler, L., Phase equilibria in the system ZrO_2–$InO_{1.5}$, *J. Am. Ceram. Soc.*, **76**(3) (1993) 689–98.
25. Stubican, V., Phase equilibria and metastabilities in the systems ZrO_2–MgO, ZrO_2–CaO and ZrO_2–Y_2O_3. In *Advances in Ceramics, Vol. 24, Science and Technology of Zirconia III*, eds S. Somiya, N. Yamamoto & H. Yanagida, American Ceramic Society, 1988, pp. 71–82.
26. Noguchi, T. & Mizuno, M., Phase change in the ZrO_2–TiO_2 System, *Bull. Chem. Soc. Jpn.*, **41**(12) (1968) 2895–9.